Optimization of Zinc Oxide Nanoparticles Biosynthesis from Morin Hydrate Using Box–Behnken Design for Enhanced Antioxidant and Antimicrobial Activity

Adeep Kujur* and Sanjay J. Daharwal
University Institute of Pharmacy, Pt. Ravishankar Shukla University, Raipur, Chhattisgarh, India 492010.
***Corresponding Author:**
***Adeep Kujur**
Assistant Professor
University Institute of Pharmacy,
Pt. Ravishankar Shukla University, Raipur, Chhattisgarh, India 492010
Contact No: +918103599558
E-mail: adeepkujuruiop@gmail.com

Co-Author:
Dr. Sanjay J. Daharwal
Associate Professor
University Institute of Pharmacy,
Pt. Ravishankar Shukla University, Raipur, Chhattisgarh, India 492010
Contact No: +919340170550
E-mail: sjdaharwal@gmail.com

Abstract:

In the present study, synthesis of zinc oxide nanoparticles (ZnONPs) through Morin Hydrate by a novel eco-friendly, rapid and easy biological method was investigated. Morin Hydrate is recognized as a major constituent of many herbs and fruits like *Psidium Guajava* (Indian guava), almond (*Prunusdulcis*), fig (*Chlorophora Tinctoria*). The methanolic stock solution of Morin Hydrate was prepared and employed as a reducing and capping agent to synthesize stable zinc oxide nanoparticles via biological reduction approach. The method was systematically optimized using response surface methodology based Box-Behnken design (BBD), considering the effect of various independent variables (factors) such as zinc

nitrate [$Zn(NO_3)_2$] concentration, incubation time and temperature on the responses like particle size and zeta potential of synthesized zinc oxide nanoparticles. The optimum conditions were [$Zn(NO_3)_2$] (3mM), incubation time (3 hrs) and temperature (70°C). Morin Hydrate methanolic stock solution can reduces zinc ions (Zn^{++}) into zinc (Zn^0) nanoparticles (ZnONPs) within 3hrs after heating the reaction mixture (70°C) as indicated by the appeared deep yellow color. The UV-Vis spectrum of bio synthesized and optimized ZnONPs shows a characteristic strong absorption peak of Surface Plasmon Resonance (SPR) at 380 nm. Fourier transform infrared (FTIR) spectroscopy affirmed the role of Morin Hydrate as a reducing and capping agent of zinc ions. ZnONPs were subjected to X-ray diffraction (XRD) analysis, which exhibits their crystalline nature. Scanning electron microscopy (SEM) showed spherical shape, confirming the presence of elemental zinc with particle size of around 100 nm. The average particle size (z-average) was found to be 90.1 nm, its polydispersity index was 0.476 and Zeta values were measured and it was found to be -37.8 mV with the peak area of 100% intensity. This indicates that the formed zinc oxide nanoparticles (MHZnONPs) are stable. MHZnONPs were then studied for antioxidant activities by DPPH assay method, which revealed significant antioxidant activity as compared to standard antioxidant ascorbic acid. Moreover, antimicrobial potential of ZnONPs against *Staphylococcus aureus* and *Bacillus subtilis*, showed maximum zone of inhibition of 14mm, at 10 µg/mL concentration. Finally from the findings, we concluded that the synthesized ZnONPs shows excellent antioxidant and antimicrobial activity.

Keywords: Green synthesis, Zinc Oxide Nanoparticles, Response surface methodology, Box-Behnken Design, Antioxidant, Antimicrobial.

DOINumber:10.14704/nq.2022.20.8.NQ44941 **NeuroQuantology 2022; 20(8): 9199-9227**

1. Introduction

Modern biological research greatly benefits from the use of nanotechnology [1, 2]. Numerous industries, including pharmaceuticals, drug delivery, gene therapy, food, and environmental health, are using nanotechnology [3]. Due to its affordability, non-toxicity, and environmental friendliness, green mediated production of metal nanoparticles has attracted increased interest in recent years [4, 5]. Various plant elements, including the seed, stem, flower, leaf, and fruit skin, were used to synthesize nanoparticles. Green synthesized nanoparticles from plant extracts are beneficial for cosmetics and drug delivery purpose [6]. Due to their high surface-to-volume ratio and nano-scale particle sizes, metal nanoparticles derived from plants have a great antimicrobial impact and stick to microbial membranes with ease [7, 8]. Silver, copper, and zinc are the most popular green-synthesized metal nanoparticles utilized as an antimicrobial agent for medicinal purposes due to their effectiveness and safety [9, 10].

Nanomaterials with small particle sizes and large surface areas have potential in various industrial fields such as food packaging industry, cosmetics, medicine and catalysts. One of the many studies carried out thus far is metal oxide nanoparticle preparation, such as zinc oxide (ZnO), titanium dioxide (TiO_2), and silver oxide (Ag_2O). ZnO nanoparticles have receive considerable attention because of their good conductivity, chemical and physical stability, photonic and optoelectronic properties, high catalytic activity, and antibacterial, antifungal, and intensive ultraviolet (UV) and infrared (IR) filtering properties [11-14]; therefore, they are considered for biological applications such as antimicrobial agents, drug delivery, and

bioimaging probes [15], making ZnO nanoparticles interesting to synthesise. Zinc oxide (ZnO) is a large band n-type semiconductor with a hexagonal phase of wurtzite-type structure [16]. Zinc oxide nanoparticles are an ideal candidate for biological applications because of their ease manufacturing and non-toxicity [17, 18]. They already serve as a conservative alternative in food packaging [19, 20], in sunscreens thanks to their transparency in visible light and their high UV absorption capacity [21, 22], and as well as a component in antibacterial drugs and cosmetics such as deodorants [23] due to their antibacterial and antifungal potential and their effectiveness against spore, resistant bacteria and Fungi [24, 25].

In recent years, nanotechnology showed great potential for effective delivery of new molecules having pharmacokinetic problems in several preclinical studies and demonstrated the delivery of desired concentration to the different sites of action in the brain, despite of complex anatomy of the brain and the unresolved mechanics of the central nervous system. Nanoparticles with appropriate surface modifications can deliver drugs of interest beyond the BBB for diagnostic and therapeutic applications in neurological disorders, such as Alzheimer disease [26]. Moreover; the metal based nanoparticles have the ability to inhibit oxidative stress via a redox reaction. Previous studies show that zinc oxide nanoparticles are useful in neurodegenerative disease therapy and diagnosis [27].

ZnO nanoparticles are multi-purposes material with a wide range of applications and can be synthesized by several methods, such as physical and chemical methods. A novel method to synthesize ZnO nanoparticles is biological method that uses plant extracts as the reducing and capping agents. Plant extracts are superior agents for synthesizing nanoparticles because they are free from toxicants and provide essential phytochemical substances as reductor and capping agents. Enzyme, protein, flavonoid, polysaccharide, and phenol in the plant extract play an important role in the reduction process of particle. Other studies also proved that polyphenol is the main substances that influenced the formation and stabilization of nanoparticles. Compared to physical and chemical routes, biological method is an efficient and eco-friendly method because of the relatively mild operating condition [28, 29].

Morin hydrate (3,5,7,2′ ,4′ -pentahydroxyflavone) is a natural bioflavonoid, a yellow crystalline polyphenolic compound and a constituent of many herbs, vegetables and fruits like *Psidium Guajava* (Indian guava), almond (*Prunusdulcis*), fig (*Chlorophora Tinctoria*) and other Moraceae family plants which are extensively used as food and traditional herbal medicine [30]. Various research reports have shown antioxidant [31], anti-inflammatory [32], and anti-proliferative [33, 34, 35], antiarthritic, antifertility, antiplasmodic [36, 37, 38], antimicrobial [39, 40, 41], antiviral [42] effects of Morin hydrate *in-vivo* and *in-vitro*. It is also used in cardiovascular diseases and diabetes mellitus [43, 44]. This flavonoid has been reported to induce apoptosis in leukemia, prostate cancer, colon cancer, breast cancer, hepatocellular carcinoma and human oral squamous carcinoma [45, 46, 47].

In the current study, we aimed to synthesize stable zinc oxide nanoparticles (ZnONPs) utilizing Morin hydrate by biological reduction technique. The investigation focused on Box-Behnken Design (BBD) of response surface methodology (RSM) based optimization of numerous experimental parameters involved in the green synthesis of ZnONPs of morin hydrate. Different analytical techniques were used to characterize the optimized and green

synthesized ZnONPs. Optimized ZnONPs were further assessed for their antioxidant potential and antimicrobial activity against four human bacterial pathogens.

2. Materials and Methods

2.1. Materials

Zinc nitrate and plant active Morin hydrate were bought from Sigma Aldrich, USA. Double distilled water and all ingredients of this research were analytical grade purchased and utilized.

2.2. Green Synthesis of Morin Hydrate zinc oxide nanoparticles (MHZnONPs)

This biological synthesis of MHZnONPs was carried out by adopting method from Aruna *et al*., 2014, Salem *et al*., 2015, Vijayakumar *et al*., 2018 and Rathinavel *et al*., 2020 with certain modifications [48-51]. However, the synthesis conditions were improved for the present reaction by adjusting a number of synthesis-related factors.

2.2.1. Preparation of stock solution of Morin Hydrate (MH)

2 mg of the drug was weighed and diluted to 20 ml with methanol. It was stored at 4°C until further use.

2.2.2. Formulation of zinc nitrate aqueous solution (3mM)

Zinc nitrate, which was measured at 0.090g, was dissolved in 100 ml of double-distilled water and stored in an amber colour container until needed. {100 ml of $Zn(NO_3)_2 .6H_2O$ (molar mass 297.49 g·mol^{-1}, odorless, density 2.065 g/cm^3, boiling point 131 °C)} {Molarity is moles per liter. As $Zn(NO_3)_2 .6H_2O$ has a molar mass of 297.49 g/mol, a 1 M solution of $Zn(NO_3)_2 .6H_2O$ in 1 liter would be 297.49 g [1 mole of $Zn(NO_3)_2 .6H_2O$]. A total of 0.180 g of zinc nitrate is used to make 200ml of solution.}.

2.2.3. Synthesis of zinc oxide nanoparticles (MHZnONPs)

A conical flask was used to hold 5 ml of the Morin Hydrate's methanolic stock solution. A magnetic stirrer coupled to a heated plate was used to stir the mixture. Using a peristaltic pump (dropper/ syringe), 50ml of 3mM $[Zn(NO_3)_2]$ solution was added to the above stock solution drop by drop over the period of 30 seconds with 120 rpm constant stirring. The solution was heated at a temperature range of 60-80°C. The high purity phytoconstituent will act as both reducing agent and stabilizing agent of aqueous zinc nitrate. The pH of the solution mixture was adjusted to 6. The reduction process of zinc ions (Zn^{++}) to zinc (Zn^0) nanoparticles was identified and checked periodically. The colour change of the medium from colorless to deep yellow after 3 hours was observed which indicated the formation of zinc oxide nanoparticles. It revealed that aqueous zinc ions may be reduced to exceptionally stable zinc oxide nanoparticles using a methanolic stock solution of Morin hydrate.

2.2.4. Separation of zinc oxide nanoparticles

The synthesized zinc oxide nanoparticles were subsequently allowed to cool at room temperature and the supernatant was discarded. The precipitate was separated from the reaction solution by centrifugation at 8000 rpm at 60°C for 15 min after thorough washing with distilled water followed by methanol to remove the unwanted impurities and pellet was collected. Crude pellets were then resuspended in sterile double distilled water and filtered through 0.2 µm filter. Then, the obtained purified precipitant was dried using a hot air oven operating at 80 °C for 2 hours. A light yellow colored powder was obtained and this was carefully collected, preserved and stored at 4°C in air-tight bottles prior to their MHZnONPs characterization studies.

2.3. Box-Behnken Design based optimization of ZnONPs synthesis

Box-Behnken Design of RSM (Design Expert software, Trial version 12.0.3.0) was used to optimize the process parameters involved in the green mediated production of ZnONPs. Optimization of ZnONPs synthesis using BBD was achieved by considering three experimental variables involved in green synthesis of ZnONPs such as [$Zn(NO_3)_2$] concentration (A), incubation time (B) and temperature (C). These three factors were analyzed based on Box-Behnken Design done at three different levels: -1, 0 and +1 for low, medium and high levels. A total of 17 experimental trials were suggested by the selected design. Particle size (nm) and zeta potential (mV) of synthesized ZnONPs were analyzed as responses. After putting the data in BBD, mathematical modelling was performed to analyze the results. Quadratic second-order model was selected and the data-fitting with the model was analyzed by ANOVA along with other parameters like coefficient of correlation (r^2), adjusted r^2, predicted r^2 and predicted residual sum of squares. Optimized parameters needed for ZnONPs production were determined by the numerical desirability function and graphical optimization techniques. Finally BBD helps in investigating linear, quadratic model of these factors for the enhanced green synthesis of ZnONPs using plant active morin hydrate, each variable diverse at these levels which also includes three center points for replication.

2.4. Characterization of Zinc Oxide Nanoparticles

2.4.1. Determination of Particle Size Including Zeta Potential Analysis

The mean particle size (z-average), polydispersity index (PI) and zeta potential of MHZnONPs was measured by dynamic light scattering technique using Malvern Panalytical Ltd. Zeta sizer, UK (Model no. – ZSU 3200). The oven-dried powder was dissolved in water before to measurement in order to get the correct scattering intensity.

2.4.2. UV-Visible Spectroscopy

UV-visible absorption spectroscopy has been used to evaluate the optical properties of nanoparticles. The parameters employed in the green-mediated manufacture of zinc oxide nanoparticles were optimized using the Box-Behnken design, and the synthesised MHZnONPs were validated using UV-Visible spectroscopy by using the Systronics UV-2201 PC scanning double beam spectrophotometer device. Using distilled water as a blank, the UV-Visible spectrum was recorded in the transmittance region of 200-800 nm, and the green production of ZnONPs was seen by a rise in absorbance.

2.4.3. Fourier Transform-Infrared (FT-IR) Spectroscopy Analysis

To identify the functional groups of biomolecules present in the nanoparticles, FTIR analysis of biologically synthesized ZnONPs was carried out. This study was performed using KBr pellet method, between the ranges of 400-4000 cm^{-1}, at room temperature. Briefly stated, the sample was combined with KBr powder and compacted into a pellet with a manual tablet presser. Then obtained pellet was analyzed using Bruker Corporation (USA) model FTIR instrument.

2.4.4. Powder X-ray Diffraction (XRD) Measurement

The powdered sample of synthesized zinc oxide nanoparticles was put on a glass substrate and examined using XRD equipment. The XRD patterns with diffraction intensity versus 2θ were recorded using Bruker Corporation (USA) model XRD instrument, of Cu-Ka radiation with a wavelength (k) of 1.54 A° at a tube voltage of 40 kV and a tube current of 30 mA.

2.4.5. Scanning Electron Microscopy (SEM) Analysis

Newly synthesized ZnONPs was subjected to scanning electron microscopy (SEM) analysis by using EM-30 (COXEM SEM-3000, South Korea make) SEM instrument. The thin films of zinc oxide nanoparticles sample powder were created by dropping a little quantity of the sample onto the carbon-coated grid, blotting away the excess with blotting paper, and then drying for SEM study.

2.5. Antioxidant Activity of Zinc Oxide Nanoparticles

The ability of Morin hydrate zinc oxide nanoparticles (MHZnONPs) to scavenge the free radicals was examined by the DPPH (2, 2-diphenyl-1-picrylhydrazyl) spectrophotometric assay, by adopting a standard procedure [52]. A given volume (2 ml) of the zinc oxide nanoparticle solution at varying concentrations ranging from 10 - 800 µg/ml each was mixed in cuvette with 1 ml of 0.5 mM DPPH (in methanol). At room temperature the absorbance at 517 nm was measured in the dark after 30 minutes of incubation. This analysis is studied in triplicates. Antioxidant activity was computed through following equation:

% Antioxidant Activity [AA] = 100 – [{(Abs sample – Abs blank) X 100}/Abs control].

Methanol (1.0 ml) plus 2.0 ml of Morin hydrate zinc oxide nanoparticles (MHZnONPs) solution was used as the blank, while as the negative control, 1.0 ml of the DPPH solution (0.5 mM) with methanol (2 ml) was used. In the experiment, ascorbic acid served as a reference standard as well.

2.6. Antimicrobial Potential of Synthesized ZnONPs

Agar well diffusion technique was utilized to test the antimicrobial ability of green synthesized Morin hydrate ZnONPs. Green synthesized zinc oxide nanoparticle's antibacterial effect has been linked to their high surface-to-volume ratio, fine tuning nanoparticles size with their bioactive molecules of plant, which enables intimate interaction with microbial membranes. The overnight inoculated bacterial cultures of *Staphylococcus aureus* (ATCC 25923), *Bacillus subtilis* (ATCC 19659), *Escherichia coli* (ATCC 25922) and *Pseudomonas aeruginosa* (ATCC 27853) bacteria were used as the test organisms and each organism is seeded in a separate sterile petriplates using spread plate technique. For agar well diffusion circular wells (6 mm) were made. Then it was loaded with a standard drug ampicillin (10 µg/ml) and the other wells were loaded with samples such as dummy zinc oxide nanoparticles as positive control [$Zn(NO_3)_2$] (10 µg/ml), pure drug Morin hydrate (10 µg/ml), Morin hydrate loaded zinc oxide nanoparticles (10 µg/ml) and distilled water, as a negative control. After that, plates were kept in triplicate for each culture and incubated overnight at 37 degrees, and the results were recorded.

3. Results and Discussion

3.1. Box-Behnken Design Based Optimization of Zinc Oxide Nanoparticle Synthesis

The optimum conditions for the synthesis of ZnONPs were found using Box-Behnken Design. The optimization strategy is displayed in Table 1. The ANOVA of the quadratic regression model (Table 2) reveals that it was a very significant model for the two experimentally observed responses, particle size and zeta potential, as was evident from the Fisher's F-test with a very low probability value (F value ¼ 85.39 and 22.28 for particle size and zeta potential respectively). Values of 'Prob > F' (< 0.0001 for particle size and 0.0002 for zeta potential) indicate that the term of the model was significant. The Model F-values of 85.39 and 22.28 implies that the model was significant. There was only a 0.01% (for particle size) and 0.02% (for zeta potential) chance that

a model F-values will occur owing to noise. The predicted R^2 (0.8557 and 0.6755) and adjusted R^2 (0.9794 and 0.9229) values for ZnONPs synthesis were in reasonable agreement with the values of R^2 (0.9910 and 0.9663 for particle size and zeta potential respectively), which are closer to 1.0, indicating the better fitness of the model in the experimental data. In the current study, three distinct tests, including sequential model sum of squares, lack of fit tests, and model summary statistics, were run on the model for Morin hydrate-mediated synthesis of ZnONPs.

Table 1 - Box-Behnken Design for the three different factors of ZnONPs synthesis and their experimental observed responses.

	Run	Factor 1 Zinc Nitrate Conc. (mM)	Factor 2 Incubation Time (hrs)	Factor 3 Temperature (°C)	Response 1 Particle Size (nm)	Response 2 Zeta Potential (mV)
1	1	3	3	70	90.1	-37.8
5	2	3	5	60	115.44	-34.3
7	3	3	5	80	120.22	-32.1
3	4	3	7	70	135.67	-31.6
11	5	5	3	80	492.24	-26.2
9	6	5	3	60	445.44	-26.8
17	7	5	5	70	523.87	-28.1
16	8	5	5	70	525	-27.3
14	9	5	5	70	526.36	-28.5
13	10	5	5	70	523.76	-25.4
15	11	5	5	70	526.88	-28.8
10	12	5	7	60	683.36	-22.4
12	13	5	7	80	642.81	-23.2
2	14	7	3	70	485.52	-25.4
6	15	7	5	60	844.28	-19.9
8	16	7	5	80	855.23	-18.1
4	17	7	7	70	950.09	-16.7

Table 2 - Analysis of variance (ANOVA) for the response surface quadratic model from BBD.

PS	**Source**	**Sum of Squares**	**df**	**Mean Square**	**F-value**	**p-value**	
	Model	1.091E+06	9	1.212E+05	85.39	< 0.0001	Significant
	Std. Dev.	37.67	**R^2**	0.9910	**C.V. %**	7.55	
	Mean	499.19					
ZP	**Source**	**Sum of Squares**	**df**	**Mean Square**	**F-value**	**p-value**	
	Model	481.78	9	53.53	22.28	0.0002	Significant
	Std. Dev.	1.55	**R^2**	0.9663	**C.V. %**	5.82	
	Mean	-26.62					

Figures 1 and 2 depict the graphically rendered 3D plots and contour diagram, respectively. The findings show that the [$Zn(NO_3)_2$] concentration (mM), incubation time (hrs), and temperature (°C), which were optimized for ZnONPs production using plant active Morin hydrate, had a significant relationship. The optimum levels of the variables were obtained by utilizing BBD. The model predicted a desired particle size and zeta potential values appearing after [$Zn(NO_3)_2$] concentration (3 mM), incubation time (3 hrs), temperature (70 °C), were optimized for ZnONPs production. Supposed model is validated and analysis was performed under these optimal conditions. The supposed model readings were almost matched with the values measured in these experiments, thus mitigating the validity of the response model and the necessity for optimal conditions. The factors that were used to optimize the synthesis of zinc oxide nanoparticles were depicted in graphs.

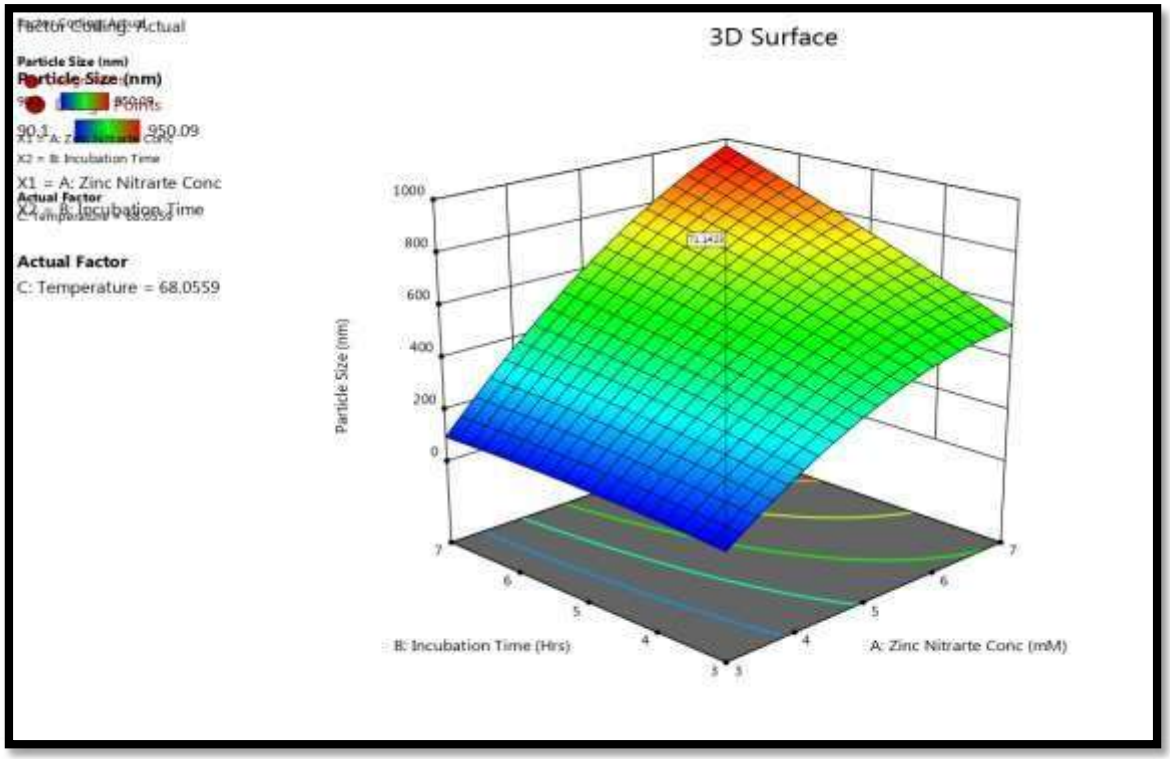
Factor Coding: Actual
Particle Size (nm)
Particle Size (nm)
950.09
90.1
X1 = A: Zinc Nitrarte Conc
X2 = B: Incubation Time
Actual Factor
C: Temperature = 68.0559
3D Surface
Particle Size (nm)
1000
800
600
400
200
0
B: Incubation Time (Hrs)
A: Zinc Nitrarte Conc (mM)

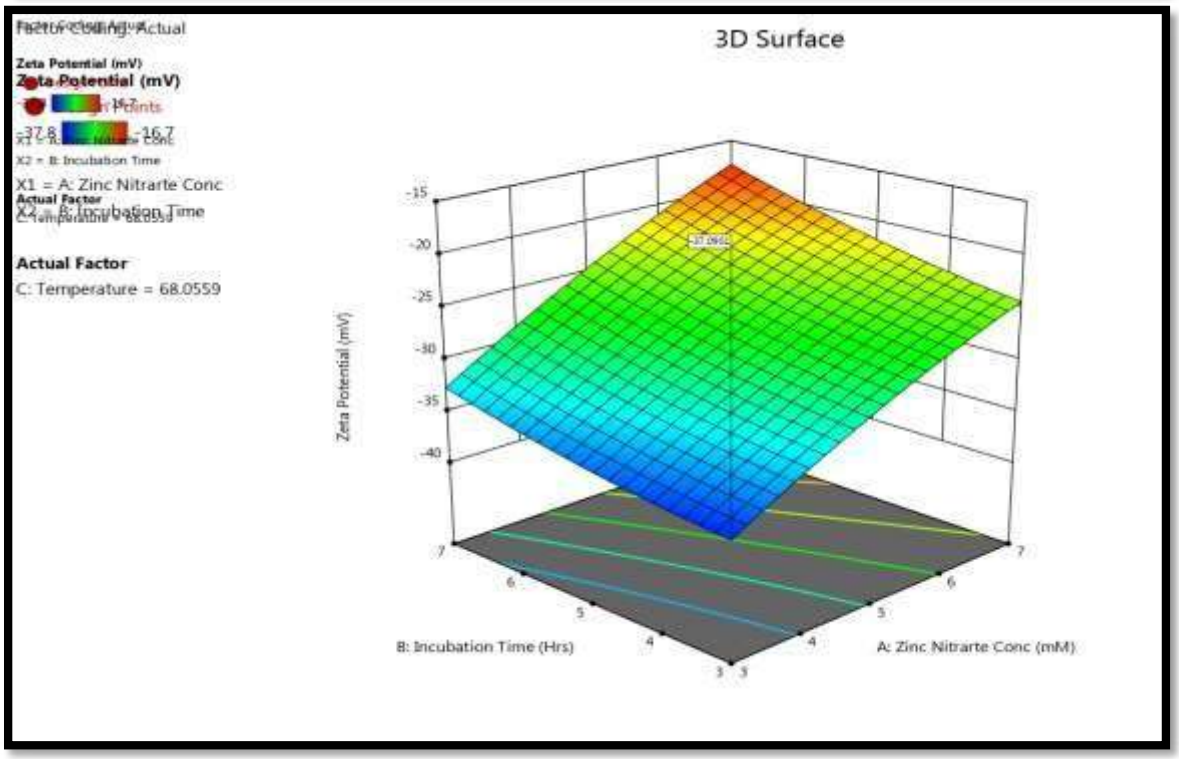
Factor Coding: Actual
Zeta Potential (mV)
Zeta Potential (mV)
-16.7
-37.8
X1 = A: Zinc Nitrarte Conc
X2 = B: Incubation Time
Actual Factor
C: Temperature = 68.0559
3D Surface
Zeta Potential (mV)
-15
-20
-25
-30
-35
-40
B: Incubation Time (Hrs)
A: Zinc Nitrarte Conc (mM)

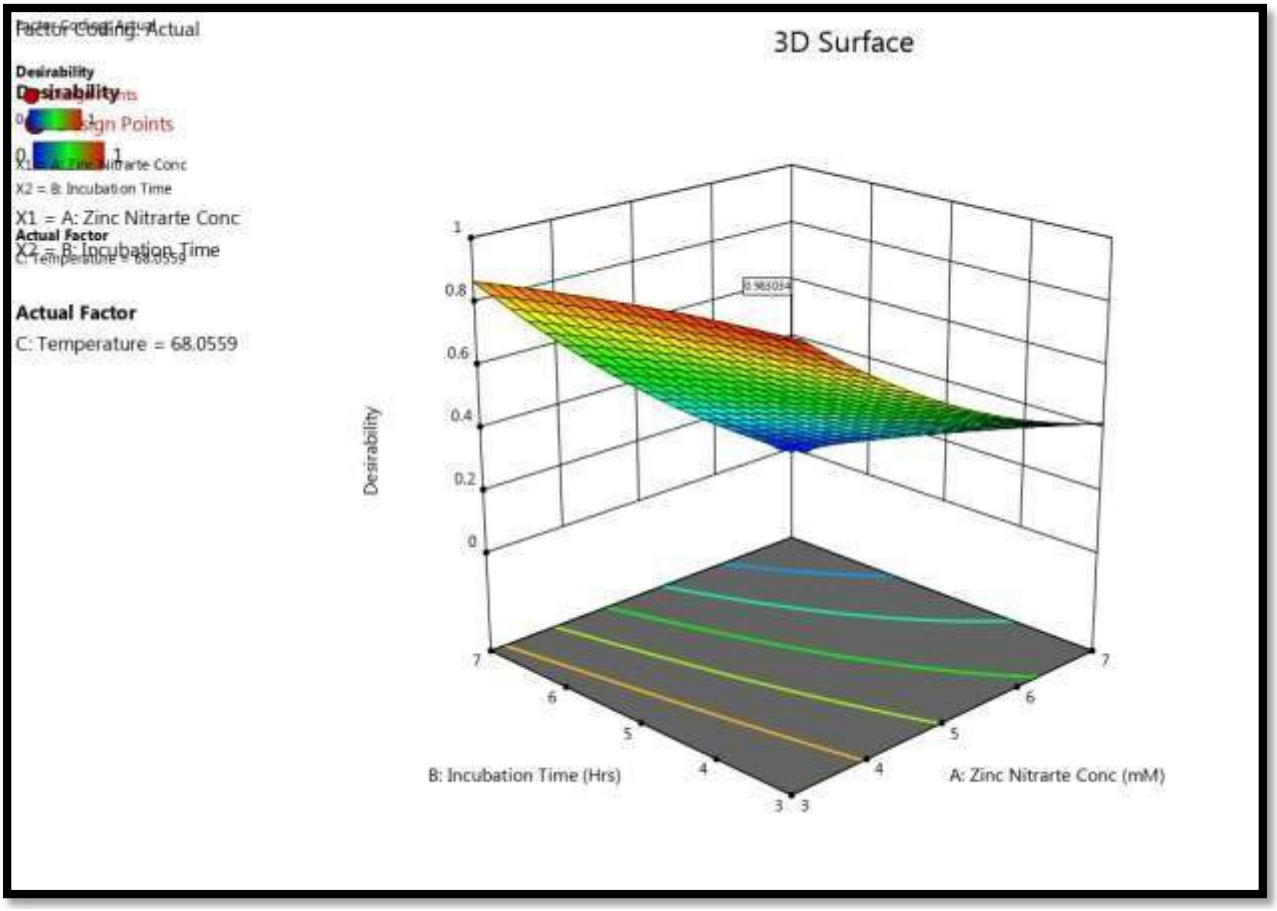

Fig. 1 3D plots showing the combined effects of two factors on biosynthesis of ZnONPs from Morin hydrate.

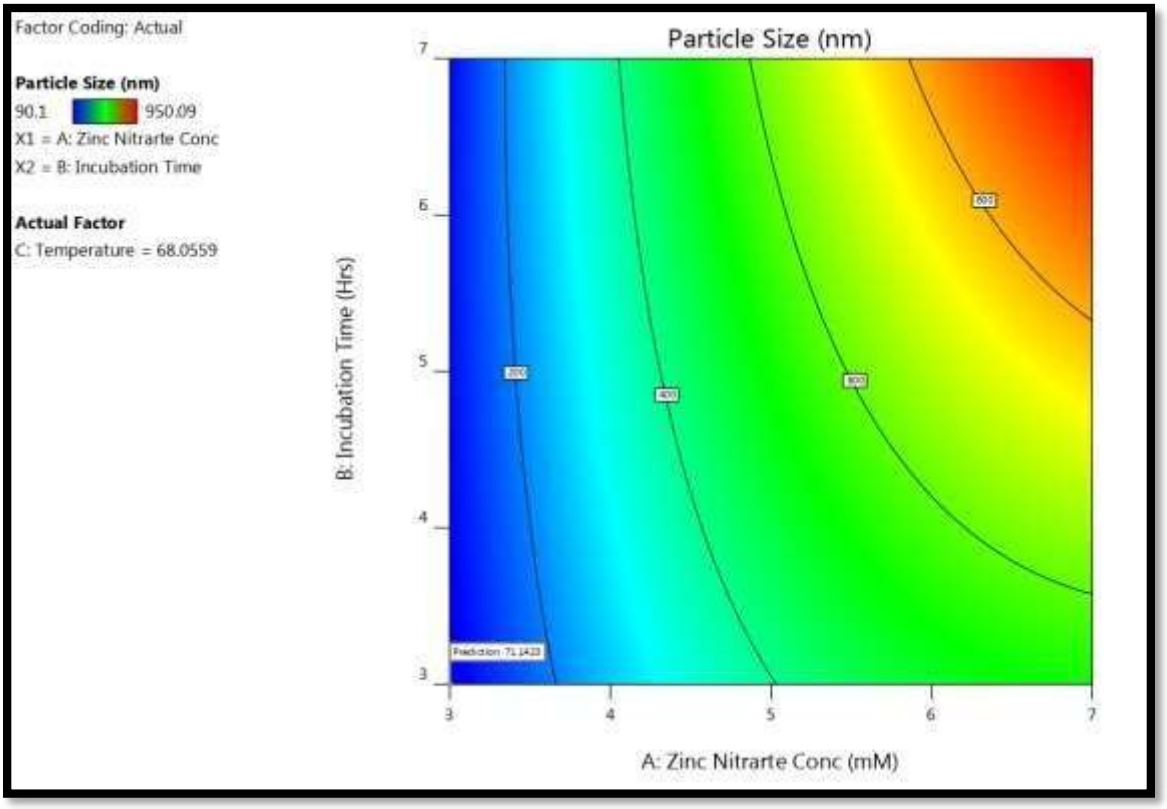
Factor Coding: Actual
Particle Size (nm)
90.1
950.09
X1 = A: Zinc Nitrarte Conc
X2 = B: Incubation Time
Actual Factor
C: Temperature = 68.0559
Particle Size (nm)
B: Incubation Time (Hrs)
A: Zinc Nitrarte Conc (mM)
3
4
5
6
7

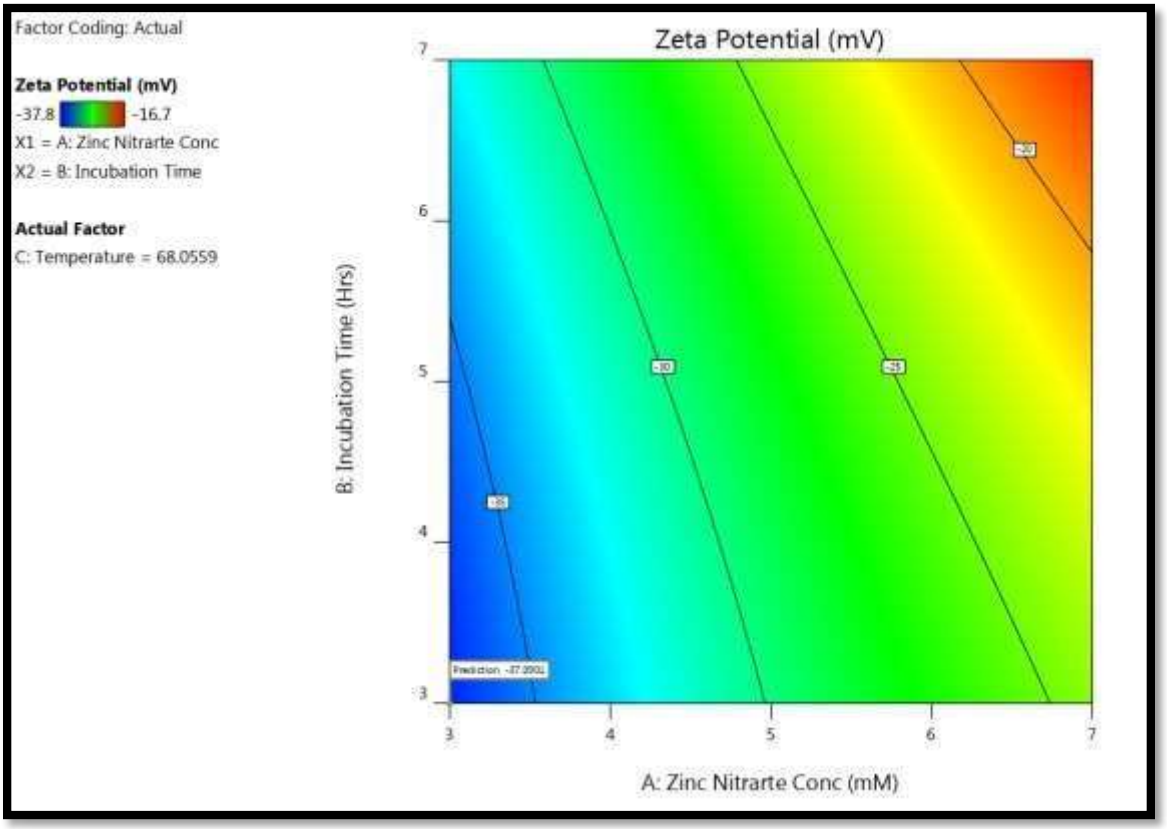
Factor Coding: Actual
Zeta Potential (mV)
-37.8
-16.7
X1 = A: Zinc Nitrarte Conc
X2 = B: Incubation Time
Actual Factor
C: Temperature = 68.0559
Zeta Potential (mV)
B: Incubation Time (Hrs)
A: Zinc Nitrarte Conc (mM)
3
4
5
6
7

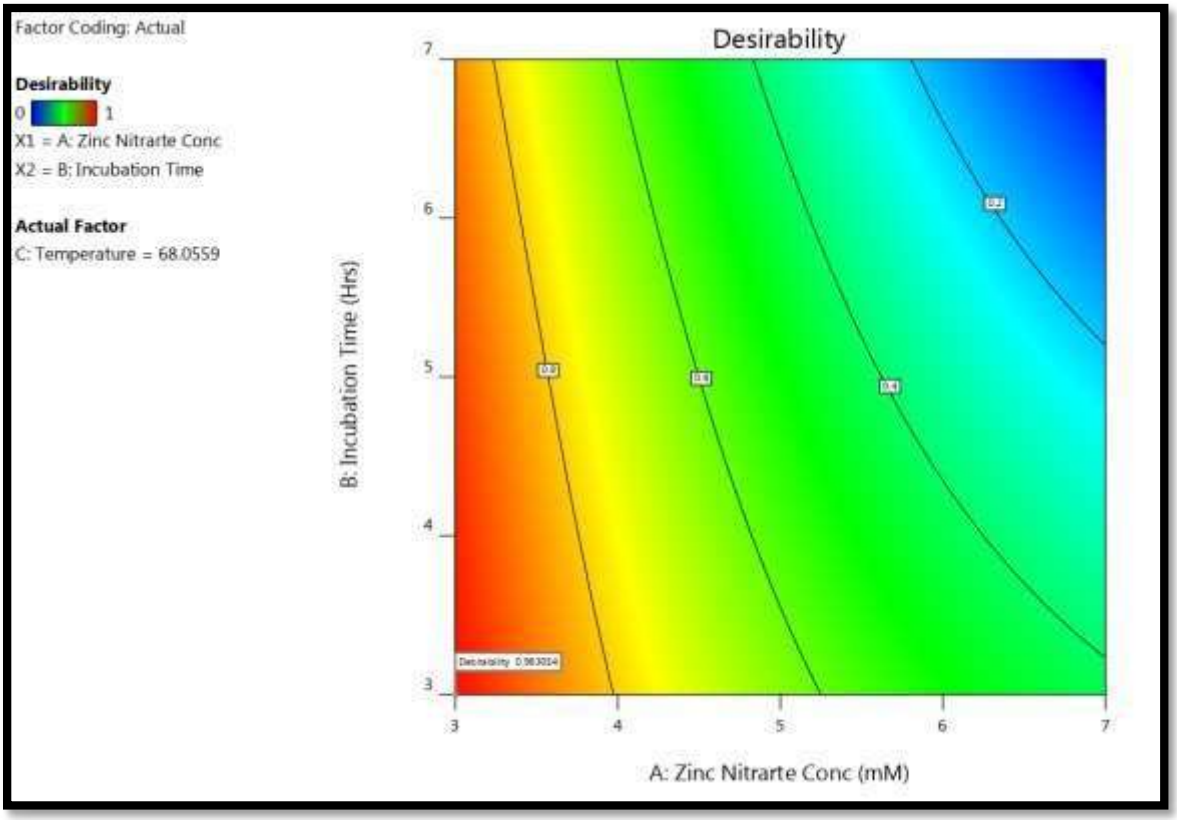
Factor Coding: Actual
Desirability
0
1
X1 = A: Zinc Nitrarte Conc
X2 = B: Incubation Time
Actual Factor
C: Temperature = 68.0559
Desirability
B: Incubation Time (Hrs)
A: Zinc Nitrarte Conc (mM)
3
4
5
6
7

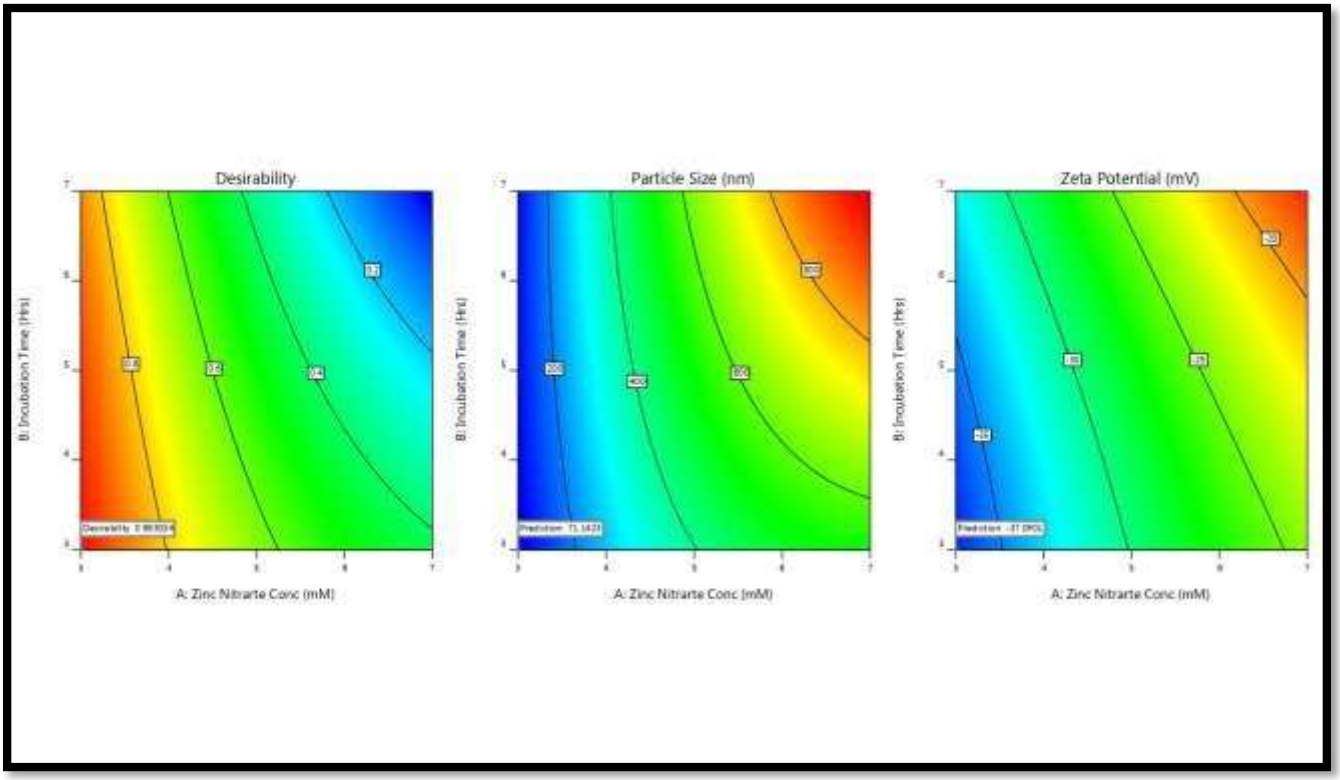

Fig. 2 2D Contour diagram for the enhanced green mediated synthesis of ZnONPs from Morin hydrate.

The following regression equation was generated by calculating the coefficients of the regression equation for Particle Size (Response 1) and Zeta Potential (Response 2), respectively:
For Particle Size (Response 1):-
Y (particle size was found to be 90.1 nm)
=
+525.17+334.21A+112.33B+2.75C+104.75AB+1.54AC-21.84BC-96.00A^2-13.83B^2+54.62C^2
For Zeta Potential (Response 2):-
Y (zeta potential was found to be -37.8 mV)
= -27.62+6.96A+2.79B+0.4750C+0.6250AB-0.1000AC-0.3500BC-0.8525A^2+0.5975B^2+2.37C^2

Where, Y stands for zinc oxide nanoparticle (ZnONPs) synthesis (for particle size 90.1 nm and zeta potential -37.8 mV), A is zinc nitrate [$Zn(NO_3)_2$] concentration, B is incubation time, C is temperature, respectively. The observed values have good similarity, thus tends to the precision and applicability of response surface methodology (RSM), to optimize the process for zinc oxide nanoparticle synthesis [53, 54, 55].

3.2. Characterization of Green Synthesized ZnONPs

3.2.1. Particle Size determination including Zeta Potential analysis

The synthesized zinc oxide nanoparticle's particle size, size distribution, and zeta potential were significant characterizations because they regulate a number of other characteristics, such as physical stability, dissolution velocity, saturation solubility, and occasionally biological manifestations [56]. The synthesized zinc oxide nanoparticles are subjected to particle size investigations, polydispersity index (PDI) or distribution pattern measurements, and zeta

potential measurements using the Zeta Size Analyzer (ZSU 3200, Malvern Panalytical Ltd., UK).

Particle size examination: Immediately following synthesis, photon correlation spectroscopy (PCS) was used to quantify the average particle size diameter and PDI in solutions. The colloidal nanoparticle size and its granulometric spreading was examined and expressed against the number of particles and their occupied volume [17].

The mean particle size (z-average) is found to be 90.1 nm. Particle size determination results in the appearance of nanoparticles having polydispersity indices PDI value 0.476 with intercept 0.681. It is shown in Table 3 and Fig. 3 respectively.

Table 3 - Mean Particle Size Diameter and Poly Dispersity Index (PDI) of Bio-synthesized MHZnONPs.

Parameter	Value	Peak No	Peak size (d.nm)	Peak intensity (%)	Peak width (d.nm)
Z-Average (d.nm)	90.1	Peak 1	113.1	100.0	40.3
PDI	0.476	Peak 2	0.000	0.0	0.000
Intercept	0.681	Peak 3	0.000	0.0	0.000

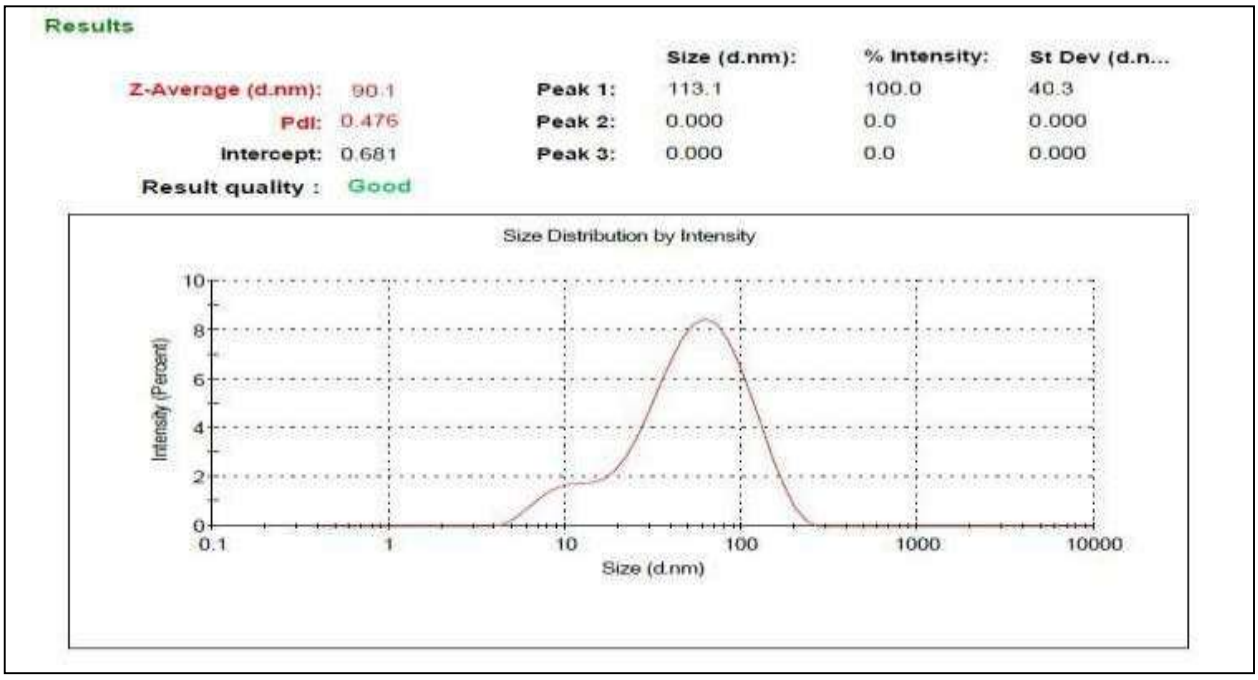

Fig. 3 Particle size distribution intensity of synthesized zinc oxide nanoparticles.

Zeta Potential Properties: The extent of surface potential of the synthesized ZnONPs was examined by zeta potential analysis. Zeta potential is a crucial indicator of the stability of aqueous ZnONPs. A zeta potential of at least +30 mV is required for the detection of stable zinc oxide nanoparticles. The zeta values of the synthesized zinc oxide nanoparticles were determined and found to be -37.8 mV with a peak area of 100% intensity [53]. These values provide total nanoparticle stability, which may be the cause of the narrow size distribution index of the synthesized particle sizes (Fig. 4).

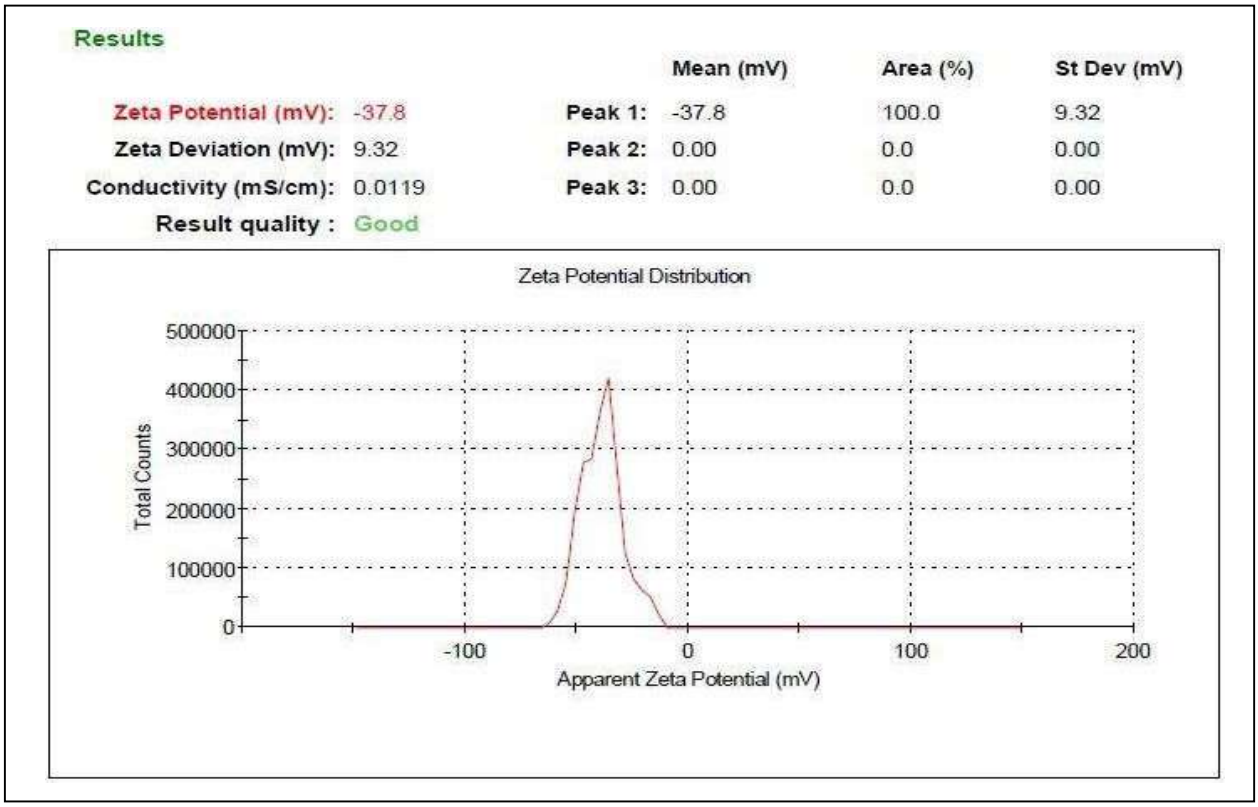

Fig. 4 Distribution of synthesized zinc oxide nanoparticles Zeta potential.

3.2.2. UV-Visible Spectroscopy

The optimized zinc oxide nanoparticle's absorption spectra were determined using UV-visible spectrophotometry, which can be seen in Figure 5. At the optimal setting of zinc nitrate concentration, incubation time and temperature, optimized zinc oxide nanoparticles were synthesized and kept at room temperature for 24 hrs. The peak of the spectrum was shown at 380 nm with a light yellow colour of the zinc oxide nanoparticle dispersion, attributed to the surface Plasmon resonance of synthesized zinc oxide nanoparticles. Moreover, the study was carried out by altering the incubation time. The observations showed that by either increasing the incubation time or temperature, absorption peaks shift towards the lower wavelength (blue shift) indicating zinc oxide nanoparticles of smaller diameter. However, zinc solution

*e*ISSN1303-5150

concentration favours the absorption peaks shift towards higher wavelength (red shift occurs), i.e., growth of zinc oxide nanoparticles of larger diameters (nucleation effects); while the sharp absorption peaks indicates formation of homogeneous zinc oxide nanoparticles [57, 58].

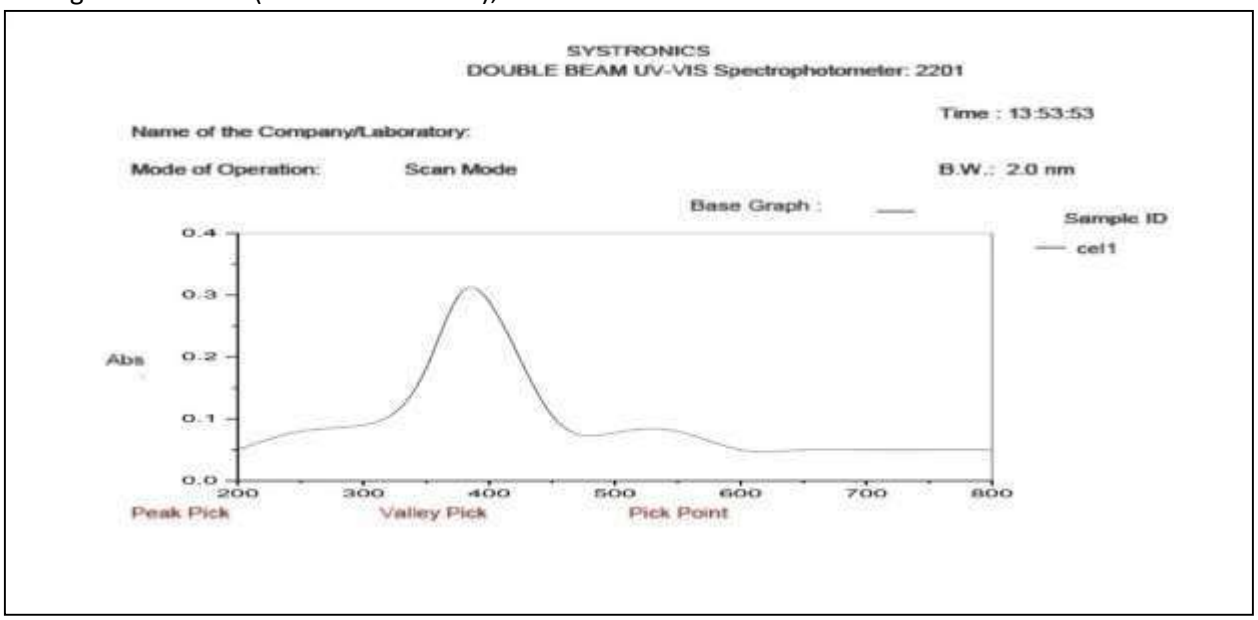

9215

Fig. 5 UV- Visible absorption spectra for Green synthesized ZnONPs from Morin hydrate.

3.2.3. Fourier Transform-Infrared (FT-IR) Spectroscopy Analysis

This study was performed to analyze the existence of functional groups responsible for reduction, capping, and hence efficient stability of the metallic nanoparticles synthesized by Morin hydrate. Figure 6 displays the FTIR spectra of Morin hydrate and its synthesized zinc oxide nanoparticles. The peak bands for the Morin hydrate in (A) observed at 3365 cm^{-1} is a characteristic of the OH stretching modes, while peak at 1662, 1603, 1524 and 1457 cm^{-1} are characteristic of C=C stretching vibration in aromatic ring and peak at 1313 cm^{-1} is for –C-OH deformation vibration and the peak 1255 and 997 cm^{-1} are for –C-OH stretching vibration. The FTIR spectra of synthesized zinc oxide nanoparticles shown in (B) indicated peak at 3345 cm^{-1} for OH stretching modes and C=C stretching vibration in aromatic ring at 1652, 1589, 1514 and 1437 cm^{-1} [59].

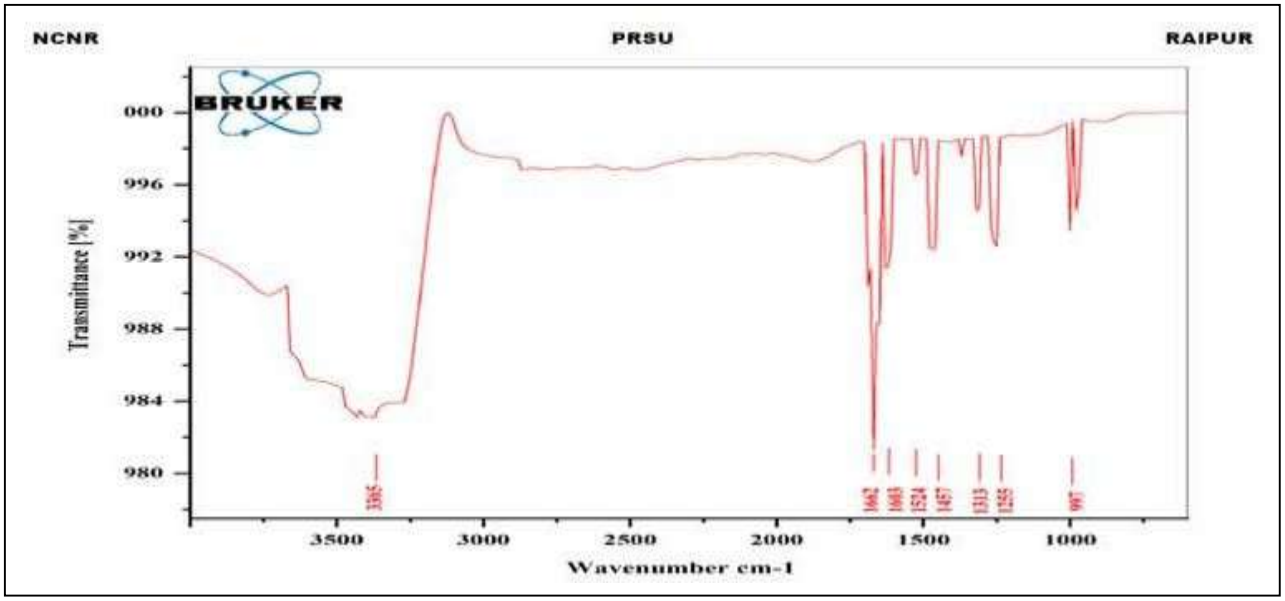

(A)

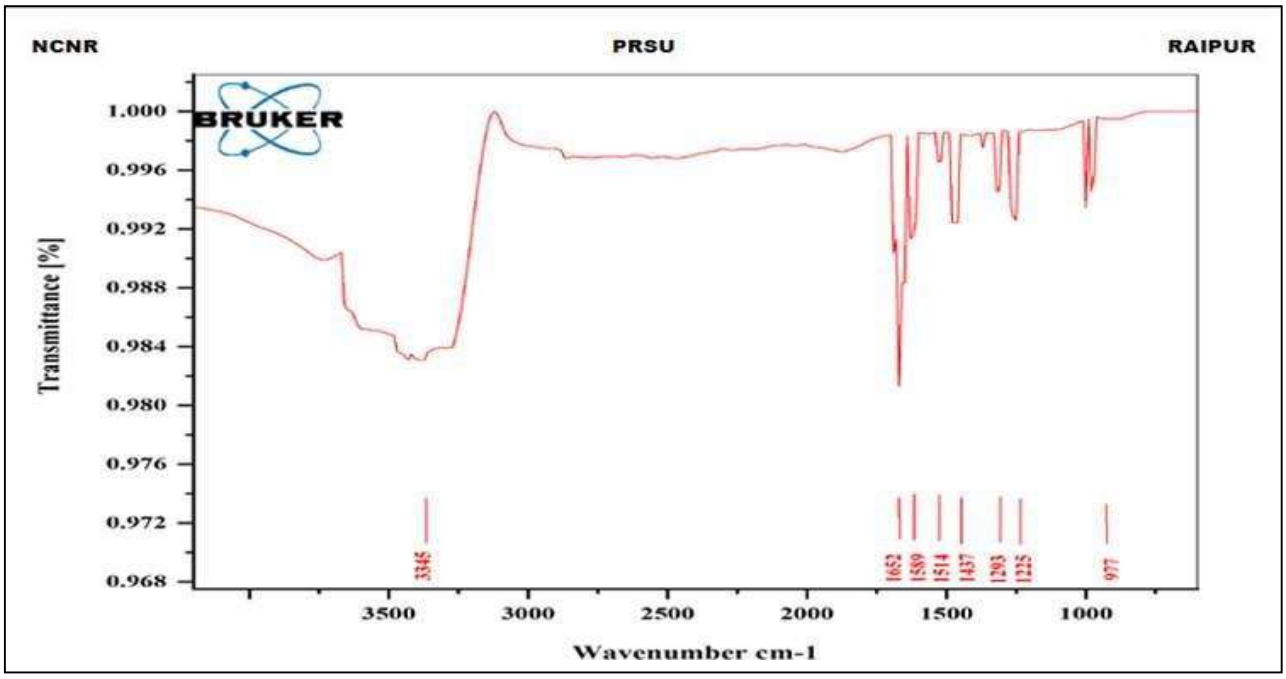

(B)

Fig. 6 (A) FTIR spectra of Morin Hydrate, (B) FTIR spectra of biosynthesized MHZnONPs.

3.2.4. Powder X-ray Diffraction (XRD) Measurement

The X-ray diffraction (XRD) patterns of freshly synthesized, oven-dried zinc oxide nanoparticles from Morin hydrate are shown in Fig. 7.

According to the XRD patterns of the ZnO/Morin hydrate, ZnONPs have a hexagonal wurtzite structure. XRD peaks at 2θ values of 32.5°, 35.6°, 37.8°, 47.4°, 57.5°, 64.7°, and 69.0° are illustrating the planes 100, 002, 101, 102,

*e*ISSN1303-5150

110, 103, 201 respectively, of the hexagonal wurtzite zinc oxide crystals. Thus, the results clearly illustrating the biosynthesis of ZnONPs and were crystalline in nature. Finally, it is concluded that the results were in accordance with the XRD patterns of standard metallic zinc oxide (JCPDS No. 36-1451). These peaks are attributable to the plant actives organic compounds, which are responsible for the reduction of zinc ions and the stability of the resulting nanoparticles [60].

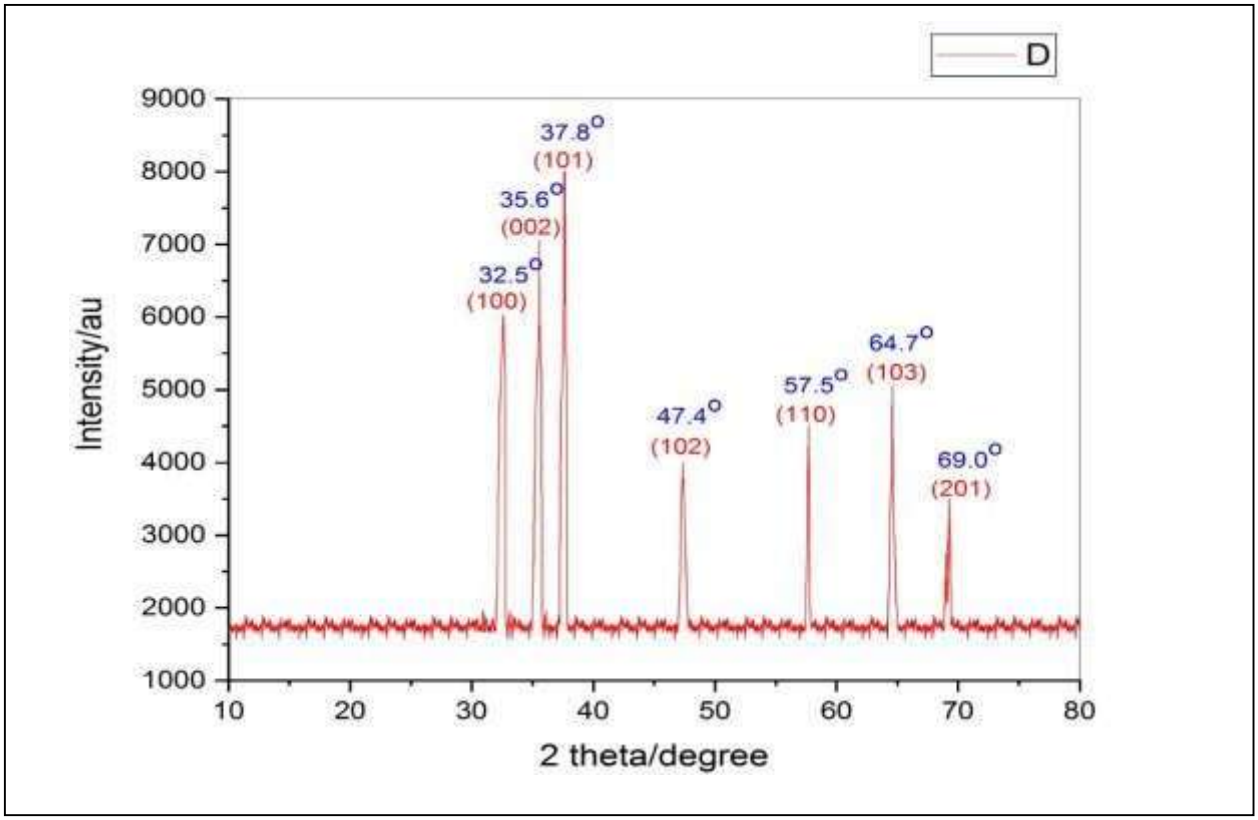

Fig. 7 XRD image of Synthesized Zinc Oxide Nanoparticles.

3.2.5. SEM (Scanning Electron Microscopy) Study

The morphology and size of the zinc oxide nanoparticles formed by the mediation of Morin hydrate using BBD were examined through SEM. The resulting micrograph picture (Fig. 8), which has an average size of around 100 nm, clearly shows the formation of spherical-shaped nanoparticles, which aggregate to form a cluster-like structure and nano crystal. SEM scans showed numerous numbers of uniformly scattered zinc oxide nanoparticles on the surface of the cells. Zinc element's presence was verified by the findings due to strong signals from zinc oxide nanoparticles like nano crystals and clusters, which demonstrated that BBD's biosynthesis of ZnONPs was effective. At the same time, the presence of zinc oxide nanoparticles in biosynthesized material was correlated with the XRD patterns [61].

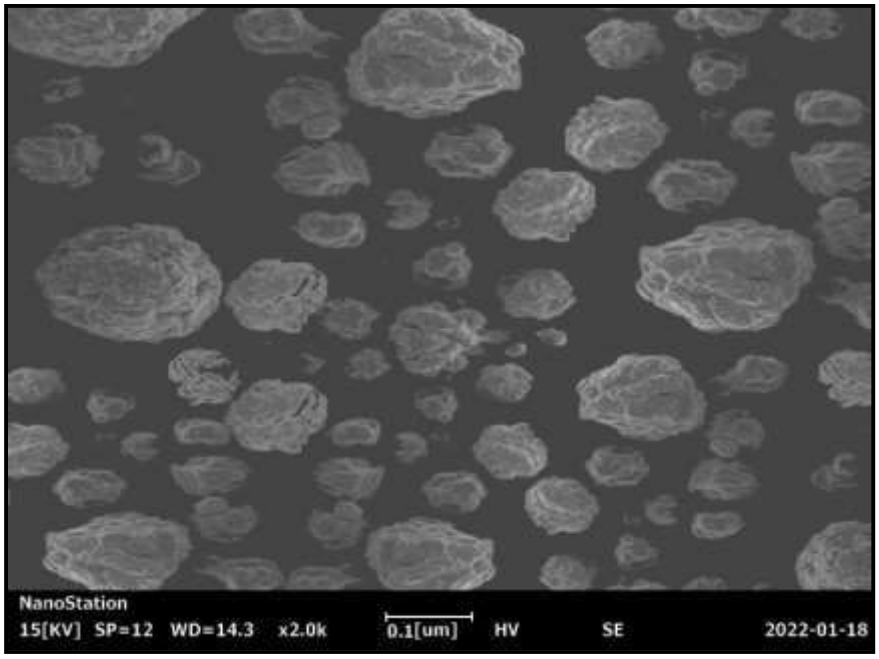

Fig. 8 SEM image of green synthesized zinc oxide nanoparticles from Morin hydrate (MHZnONPs).

3.3. Antioxidant potential of ZnONPs

Free radicals have important roles in a wide range of pathological manifestations. Antioxidants were utilized to neutralize the free radicals and stop them from spreading disease. Reactive oxygen species (ROS) scavenging or antioxidant defense mechanisms are used to accomplish this. The bleaching of purple-colored DPPH (2, 2-diphenyl-1-picrylhydrazyl radical) solution can be used to test the ability of natural products to donate electrons. The procedure works by scavenging DPPH by incorporating an antioxidant or radical species into the DPPH solution, which renders the solution colorless. The concentration and potency of the antioxidants control how strongly the color changes. The reaction mixture's absorbance is significantly reduced, indicating the substance under investigation possesses potent free radical scavenging properties. In the current investigation, when compared to ascorbic acid, the manufactured zinc oxide nanoparticles (MHZnONPs) displayed considerable antioxidant properties at high concentrations, the results revealed. When compared to the activity of 87.03 ± 0.91 % of standard ascorbic acid at the same concentration, the compound's 84.59 ± 1.15 % activity at 800 µg/ml is noteworthy (Table 4 & Fig. 9) [52, 62].

Table 4 – Antioxidant activity of synthesized ZnONPs by DPPH assay method.

Sr.No	MHZnONPs Test sample		Standard Absorbace Ascorbic Acid (µg/ml)	
	Concentration (ug/ml)	% Scavenging	Concentration (ug/ml)	% Scavenging
1.	10	38.51 ± 0.72	10	75.15 ± 0.81
2.	50	54.68 ± 1.03	50	75.76 ± 0.71
3.	100	64.45 ± 0.91	100	76.31 ± 0.88
4.	200	72.75 ± 0.66	200	79.27 ± 0.70
5.	400	76.57 ± 0.81	400	83.41 ± 0.72
6.	800	84.59 ± 1.15	800	87.03 ± 0.91

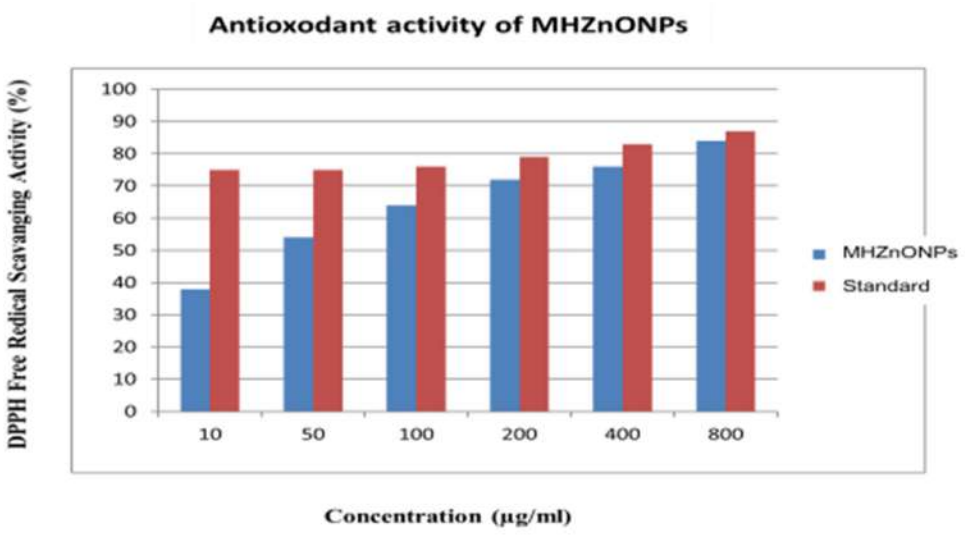

Fig. 9 Antioxidant activities of MHZnONPs as compared with ascorbic acid using the DPPH assay method.

3.4. Antimicrobial Activity of Zinc Oxide Nanoparticles

Figures 10 and 11 depict the outcomes of MHZnONP's antimicrobial activity against four human bacterial pathogenic strains. Compared to its green-synthesized zinc oxide nanoparticles (MHZnONPs), pure plant-active Morin hydrate has reduced antimicrobial activity. The results showed that MHZnONPs exhibited good antimicrobial action against *Staphylococcus*

multi drug resistance since RSM optimized ZnONPs of plant active Morin hydrate demonstrated outstanding antimicrobial. *aureus* and *Bacillus subtilis*, when compared with two other clinical pathogens. ZnONPs that have been optimized from Morin hydrate have a maximal zone of inhibition of 14 mm against *Staphylococcus aureus* and *Bacillus subtilis* at 10µg/ml concentration, although *Escherichia coli* and *Pseudomonas aeruginosa* both had a 13 mm zone of inhibition. Zone of inhibition measurements are shown in Table 5. It is helpful to treat bacteria that have developed

efficacy against human clinical pathogens like *Staphylococcus aureus* and *Bacillus subtilis* [63, 64, 65].

Table 5 - In-vitro Antimicrobial Study of synthesized Morin Hydrate Zinc Oxide Nanoparticles (MHZnONPs) and their experimental observed responses.

Name of Sample	**Observed Zone of Inhibition in various pathogens (mm)**			
	Staphylococcus Aureus	***Bacillus Subtilis***	***Escherichia Coli***	***Pseudomonas Aeruginosa***
Negative Control (Distilled Water)	0	0	0	0
Dummy Zinc Oxide Nanoparticles as Positive Control [$Zn(NO_3)_2$] (10 µg/ml)	3	3	3	3
Pure Drug Morin Hydrate (10 µg/ml)	6	6	5	6
Standard Drug Ampicillin (10 µg/ml)	16	15	17	16
Morin Hydrate loaded Zinc Oxide nanoparticles (MHZnONPs) (10 µg/ml)	14	14	13	13

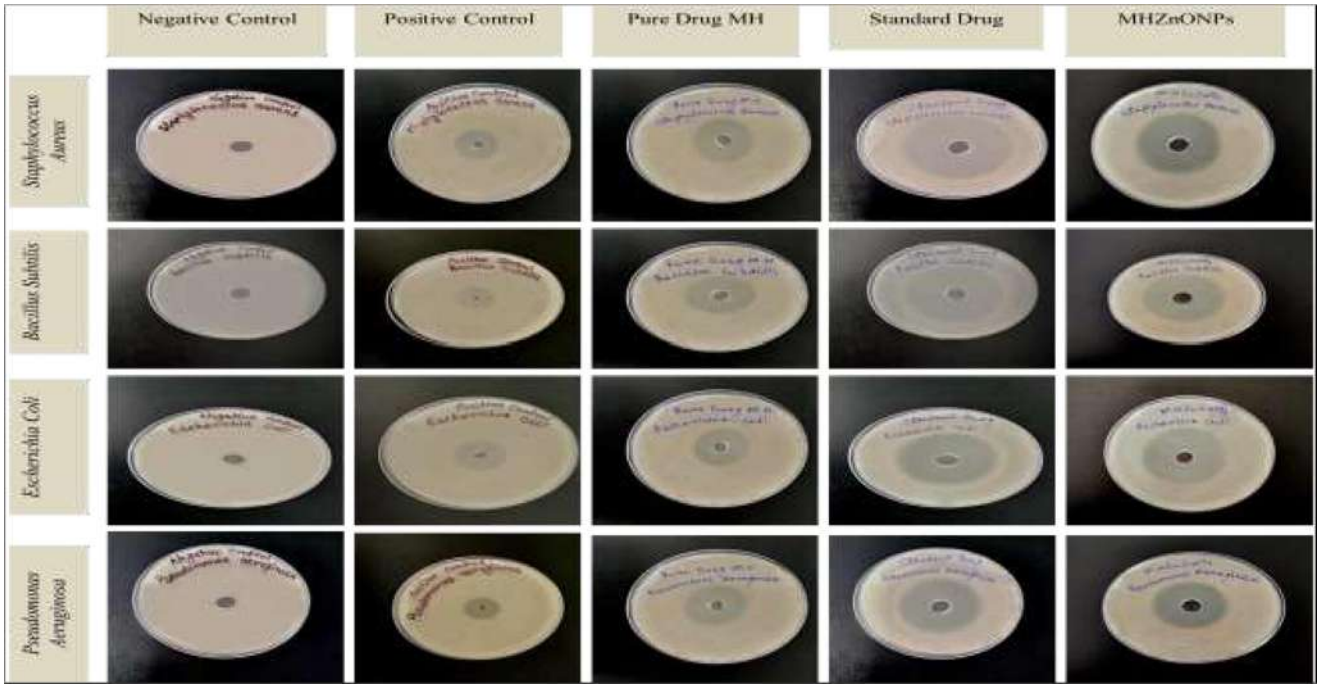

Fig. 10 Antimicrobial activity of synthesized Morin Hydrate Zinc Oxide Nanoparticles (MHZnONPs) against four different human bacterial pathogens.

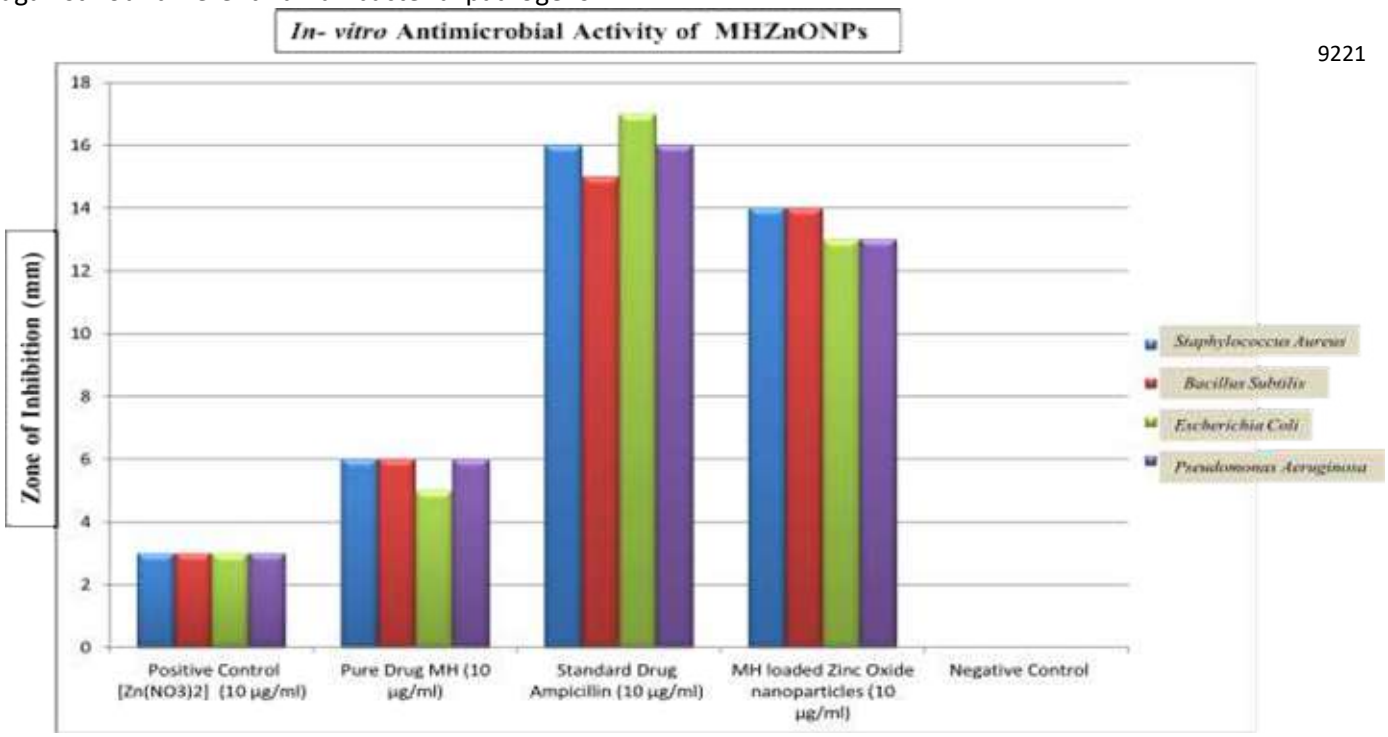

Fig. 11 Antimicrobial activity of Morin hydrate and its synthesized zinc oxide nanoparticles.

4. Conclusions

Stable zinc oxide nanoparticles were synthesized using plant active Morin hydrate, as a bioreducing and capping agent as it is simple, cost-effective, green synthesis approach based biological reduction method. Newly synthesized zinc oxide nanoparticles were systematically optimized using Box-Behnken design, considering the effect of various independent variables (factors) like concentration of [$Zn(NO_3)_2$], incubation time and temperature on the responses like particle size and zeta potential. The ZnONPs were characterized by Particle size and Zeta potential, UV-visible, FT-IR spectrum, XRD and SEM. The synthesized zinc oxide nanoparticles at optimal conditions were found to have a spherical shape under SEM with particle size of around 100 nm. The mean particle size, z-average was found to be 90.1 nm, with the polydispersity index value of 0.476. In addition, these ZnONPs were evaluated for antioxidant activities by DPPH assay method, which revealed significant antioxidant activity against standard ascorbic acid. Furthermore, these synthesized zinc oxide nanoparticles showed prominent antimicrobial activity against four human pathogens. Lastly, this investigation proves that the biologically synthesized Morin hydrate based zinc oxide nanoparticles can be a better alternative as antioxidant and antimicrobial agent.

Declaration of Competing Interest

The authors declare that there is no conflict of interest regarding the publication of this manuscript.

Acknowledgments

The authors express sincere gratitude to the University Institute of Pharmacy, Pt. Ravishankar Shukla University, Raipur, Chhattisgarh, India for their technical support.

References

[1] Ramadhan VB, Nimah YL, Yanuar E, Suprapto S. Synthesis of copper nanoparticles using Ocimum tenuiflorum leaf extract as capping Agent. In AIP Conference Proceedings 2019 Dec 27 (Vol. 2202, No. 1, p. 020067). AIP Publishing LLC.

[2] Umer A, Naveed S, Ramzan N, Rafique MS. Selection of a suitable method for the synthesis of copper nanoparticles. Nano. 2012 Oct 22;7(05):1230005.

[3] Yeo SY, Lee HJ, Jeong SH. Preparation of nanocomposite fibers for permanent antibacterial effect. Journal of Materials science. 2003 May;38(10):2143-7.

[4] He Y, Lu HT, Sai LM, Lai WY, Fan QL, Wang LH, Huang W. Synthesis of CdTe nanocrystals through program process of microwave irradiation. The Journal of Physical Chemistry B. 2006 Jul 13;110(27):13352-6.

[5] Cooper JS, Myers M, Chow E, Hubble LJ, Cairney JM, Pejcic B, Müller KH, Wieczorek L, Raguse B. Performance of graphene, carbon nanotube, and gold nanoparticle chemiresistor sensors for the detection of petroleum hydrocarbons in water. Journal of nanoparticle research. 2014 Jan;16(1):1-3.

[6] Klueh U, Wagner V, Kelly S, Johnson A, Bryers JD. Efficacy of silver-coated fabric to prevent bacterial colonization and subsequent device-based biofilm formation. Journal of Biomedical Materials Research: An Official Journal of The Society for Biomaterials, The Japanese Society for Biomaterials, and The Australian Society for Biomaterials and the Korean Society for Biomaterials. 2000;53(6):621-31.

[7] Chwalibog A, Sawosz E, Hotowy A, Szeligx a J, Mitura S, Mitura K, Grodzik M, Orlowski P, Sokolowska A. Visualization of interaction between inorganic nanoparticles and bacteria or fungi. International Journal of Nanomedicine. 2010;5:1085.

[8] Khammee P, Ramaraj R, Whangchai N, Bhuyar P, Unpaprom Y. The immobilization of yeast for fermentation of macroalgae Rhizoclonium sp. for efficient conversion into bioethanol. Biomass Conversion and Biorefinery. 2021 Jun;11(3):827-35.
[9] Gajbhiye M, Kesharwani J, Ingle A, Gade A, Rai M. Fungus-mediated synthesis of silver nanoparticles and their activity against pathogenic fungi in combination with fluconazole. Nanomedicine: Nanotechnology, Biology and Medicine. 2009 Dec 1;5(4):382-6.
[10] Ali KA, Yao R, Wu W, Masum MM, Luo J, Wang Y, Zhang Y, An Q, Sun G, Li B. Biosynthesis of silver nanoparticle from pomelo (Citrus Maxima) and their antibacterial activity against acidovorax oryzae RS-2. Materials Research Express. 2020 Jan 27;7(1):015097.
[11] Mohd Yusof H, Mohamad R, Zaidan UH, Rahman A. Microbial synthesis of zinc oxide nanoparticles and their potential application as an antimicrobial agent and a feed supplement in animal industry: a review. Journal of animal science and biotechnology. 2019 Dec;10(1):1-22.
[12] Jiang J, Pi J, Cai J. The advancing of zinc oxide nanoparticles for biomedical applications. Bioinorganic chemistry and applications. 2018 Oct;2018.
[13] Buazar F, Alipouryan S, Kroushawi F, Hossieni SA. Photodegradation of odorous 2-mercaptobenzoxazole through zinc oxide/hydroxyapatite nanocomposite. Applied nanoscience. 2015 Aug;5(6):719-29.
[14] Buazar F, Bavi M, Kroushawi F, Halvani M, Khaledi-Nasab A, Hossieni SA. Potato extract as reducing agent and stabiliser in a facile green one-step synthesis of ZnO nanoparticles. Journal of Experimental Nanoscience. 2016 Feb 11;11(3):175-84.
[15] Chauhan R, Reddy A, Abraham J. Biosynthesis of silver and zinc oxide nanoparticles using Pichia fermentans JA2 and their antimicrobial property. Applied nanoscience. 2015 Jan;5(1):63-71.
[16] Sajjad M, Ullah I, Khan MI, Khan J, Khan MY, Qureshi MT. Structural and optical properties of pure and copper doped zinc oxide nanoparticles. Results in Physics. 2018 Jun 1;9:1301-9.
[17] Jamdagni P, Khatri P, Rana JS. Green synthesis of zinc oxide nanoparticles using flower extract of Nyctanthes arbor-tristis and their antifungal activity. Journal of King Saud University-Science. 2018 Apr 1;30(2):168-75.
[18] Wu B, Wu J, Liu S, Shen Z, Chen L, Zhang XX, Ren HQ. Combined effects of graphene oxide and zinc oxide nanoparticle on human A549 cells: bioavailability, toxicity and mechanisms. Environmental Science: Nano. 2019;6(2):635-45.
[19] Espitia PJ, Soares ND, Coimbra JS, de Andrade NJ, Cruz RS, Medeiros EA. Zinc oxide nanoparticles: synthesis, antimicrobial activity and food packaging applications. Food and bioprocess technology. 2012 Jul;5(5):1447-64.
[20] Jayakumar A, Heera KV, Sumi TS, Joseph M, Mathew S, Praveen G, Nair IC, Radhakrishnan EK. Starch-PVA composite films with zinc-oxide nanoparticles and phytochemicals as intelligent pH sensing wraps for food packaging application. International Journal of Biological Macromolecules. 2019 Sep 1;136:395-403.
[21] Franklin NM, Rogers NJ, Apte SC, Batley GE, Gadd GE, Casey PS. Comparative toxicity of nanoparticulate ZnO, bulk ZnO, and ZnCl2 to a freshwater microalga (Pseudokirchneriella subcapitata): the importance of particle solubility. Environmental science & technology. 2007 Dec 15;41(24):8484-90.
[22] Mohammed YH, Holmes A, Haridass IN, Sanchez WY, Studier H, Grice JE, Benson HA, Roberts MS. Support for the safe use of zinc oxide nanoparticle sunscreens: lack of skin penetration or cellular toxicity after repeated application in volunteers. Journal of

Investigative Dermatology. 2019 Feb 1;139(2):308-15.
[23] Li Q, Mahendra S, Lyon DY, Brunet L, Liga MV, Li D, Alvarez PJ. Antimicrobial nanomaterials for water disinfection and microbial control: potential applications and implications. Water research. 2008 Nov 1;42(18):4591-602.
[24] Azam A, Ahmed AS, Oves M, Khan MS, Habib SS, Memic A. Antimicrobial activity of metal oxide nanoparticles against Gram-positive and Gram-negative bacteria: a comparative study. International journal of nanomedicine. 2012;7:6003.
[25] Obeizi Z, Benbouzid H, Ouchenane S, Yılmaz D, Culha M, Bououdina M. Biosynthesis of Zinc oxide nanoparticles from essential oil of Eucalyptus globulus with antimicrobial and anti-biofilm activities. Materials Today Communications. 2020 Dec 1;25:101553.

[26] Roney C, Kulkarni P, Arora V, Antich P, Bonte F, Wu A, Mallikarjuana NN, Manohar S, Liang HF, Kulkarni AR, Sung HW. Targeted nanoparticles for drug delivery through the blood–brain barrier for Alzheimer's disease. Journal of controlled release. 2005 Nov 28;108(2-3):193-214.
[27] Shukla R, Singh A, Handa M, Flora SJ, Kesharwani P. Nanotechnological approaches for targeting amyloid-β aggregation with potential for neurodegenerative disease therapy and diagnosis. Drug Discovery Today. 2021 Aug 1;26(8):1972-9.
[28] Rahayu E, Wonoputri V, Samadhi TW. Plant extract-assisted biosynthesis of zinc oxide nanoparticles and their antibacterial application. InIOP Conference Series: Materials Science and Engineering 2020 Apr 1 (Vol. 823, No. 1, p. 012036). IOP Publishing.
[29] Parveen K, Banse V, Ledwani L. Green synthesis of nanoparticles: their advantages and disadvantages. InAIP conference proceedings 2016 Apr 13 (Vol. 1724, No. 1, p. 020048). AIP Publishing LLC.
[30] Karamchedu S, Tunki L, Kulhari H, Pooja D. Morin hydrate loaded solid lipid nanoparticles: Characterization, stability, anticancer activity, and bioavailability. Chemistry and Physics of Lipids. 2020 Nov 1;233:104988.
[31] Shetty PK, Venuvanka V, Jagani HV, Chethan GH, Ligade VS, Musmade PB, Nayak UY, Reddy MS, Kalthur G, Udupa N, Rao CM. Development and evaluation of sunscreen creams containing morin-encapsulated nanoparticles for enhanced UV radiation protection and antioxidant activity. International journal of nanomedicine. 2015;10:6477-6491.
[32] Hogaboam CM, Jacobson K, Collins SM, Blennerhassett MG. The selective beneficial effects of nitric oxide inhibition in experimental colitis. American Journal of Physiology-Gastrointestinal and Liver Physiology. 1995 Apr 1;268(4):G673-84.
[33] Chen YC, Shen SC, Chow JM, Ko CH, Tseng SW. Flavone inhibition of tumor growth via apoptosis in vitro and in vivo. International journal of oncology. 2004 Sep 1;25(3):661-70.
[34] Jangid AK, Agraval H, Gupta N, Jain P, Yadav UC, Pooja D, Kulhari H. Amorphous nano morin outperforms native molecule in anticancer activity and oral bioavailability. Drug Development and Industrial Pharmacy. 2020 Jul 2;46(7):1123-32.
[35] Jangid AK, Agraval H, Gupta N, Yadav UC, Sistla R, Pooja D, Kulhari H. Designing of fatty acid-surfactant conjugate based nanomicelles of morin hydrate for simultaneously enhancing anticancer activity and oral bioavailability. Colloids and Surfaces B: Biointerfaces. 2019 Mar 1;175:202-11.
[36] Jangid AK, Pooja D, Kulhari H. Determination of solubility, stability and degradation kinetics of morin hydrate in

physiological solutions. RSC advances. 2018;8(50):28836-42.
[37] Zhang QF, Fu YJ, Huang ZW, Shangguang XC, Guo YX. Aqueous stability of astilbin: effects of pH, temperature, and solvent. Journal of agricultural and food chemistry. 2013 Dec 11;61(49):12085-91.
[38] Ghosh P, Bag S, Roy AS, Subramani E, Chaudhury K, Dasgupta S. Solubility enhancement of morin and epicatechin through encapsulation in an albumin based nanoparticulate system and their anticancer activity against the MDA-MB-468 breast cancer cell line. RSC advances. 2016;6(103):101415-29.
[39] Wang J, Zhou X, Liu S, Li G, Shi L, Dong J, Li W, Deng X, Niu X. Morin hydrate attenuates S taphylococcus aureus virulence by inhibiting the self-assembly of α-hemolysin. Journal of applied microbiology. 2015 Mar;118(3):753-63.
[40] Yang JY, Lee HS. Evaluation of antioxidant and antibacterial activities of morin isolated from mulberry fruits (Morus alba L.). Journal of the Korean Society for Applied Biological Chemistry. 2012 Aug;55(4):485-89.
[41] Rajput SA, Wang XQ, Yan HC. Morin hydrate: A comprehensive review on novel natural dietary bioactive compound with versatile biological and pharmacological potential. Biomedicine & pharmacotherapy. 2021 Jun 1;138:111511.
[42] Hong EH, Song JH, Kim SR, Cho J, Jeong B, Yang H, Jeong JH, Ahn JH, Jeong H, Kim SE, Chang SY. Morin hydrate inhibits influenza virus entry into host cells and has anti-inflammatory effect in influenza-infected mice. Immune Network. 2020 Aug;20(4).
[43] Gopal JV. Morin hydrate: botanical origin, pharmacological activity and its applications: a mini-review. Pharmacognosy Journal. 2013 May 1;5(3):123-26.
[44] Abuohashish HM, Al-Rejaie SS, Al-Hosaini KA, Parmar MY, Ahmed MM. Alleviating effects of morin against experimentally-induced diabetic osteopenia. Diabetology & metabolic syndrome. 2013 Dec;5(1):1-8.
[45] Kuo HM, Chang LS, Lin YL, Lu HF, Yang JS, Lee JH, Chung JG. Morin inhibits the growth of human leukemia HL-60 cells via cell cycle arrest and induction of apoptosis through mitochondria dependent pathway. Anticancer research. 2007 Jan 1;27(1A):395-405.
[46] Sivaramakrishnan V, Devaraj SN. Morin regulates the expression of NF-κB-p65, COX-2 and matrix metalloproteinases in diethylnitrosamine induced rat hepatocellular carcinoma. Chemico-Biological Interactions. 2009 Aug 14;180(3):353-9.
[47] Sivaramakrishnan V, Shilpa PN, Kumar VR, Devaraj SN. Attenuation of N-nitrosodiethylamine-induced hepatocellular carcinogenesis by a novel flavonol—Morin. Chemico-biological interactions. 2008 Jan 10;171(1):79-88.
[48] Aruna A, Nandhini R, Karthikeyan V, Bose P. Synthesis and characterization of silver nanoparticles of insulin plant (costus pictus d. don) leaves. Asian journal of biomedical and pharmaceutical sciences. 2014 Jul 1;4(34):1.
[49] Salem W, Leitner DR, Zingl FG, Schratter G, Prassl R, Goessler W, Reidl J, Schild S. Antibacterial activity of silver and zinc nanoparticles against Vibrio cholerae and enterotoxic Escherichia coli. International Journal of Medical Microbiology. 2015 Jan 1;305(1):85-95.
[50] Vijayakumar S, Mahadevan S, Arulmozhi P, Sriram S, Praseetha PK. Green synthesis of zinc oxide nanoparticles using Atalantia monophylla leaf extracts: Characterization and antimicrobial analysis. Materials Science in Semiconductor Processing. 2018 Aug 1;82:39-45.
[51] Rathinavel T, Ammashi S, Marimuthu S. Optimization of zinc oxide nanoparticles biosynthesis from Crateva adansonii using Box-Behnken design and its antimicrobial activity.

*e*ISSN1303-5150

Chemical Data Collections. 2020 Dec 1;30:100581.
[52] Mensor LL, Menezes FS, Leitão GG, Reis AS, Santos TC, Coube CS, Leitão SG. Screening of Brazilian plant extracts for antioxidant activity by the use of DPPH free radical method. Phytotherapy research. 2001 Mar;15(2):127-30.
[53] Al-Kordy HM, Sabry SA, Mabrouk ME. Statistical optimization of experimental parameters for extracellular synthesis of zinc oxide nanoparticles by a novel haloalaliphilic Alkalibacillus sp. W7. Scientific reports. 2021 May 25;11(1):1-4.
[54] Kovács Z, Molnár C, Štangar UL, Cristea VM, Pap Z, Hernadi K, Baia L. Optimization Method of the Solvothermal Parameters Using Box–Behnken Experimental Design—The Case Study of ZnO Structural and Catalytic Tailoring. Nanomaterials. 2021 May;11(5):1334.
[55] Mulyani F, Permana MD, Ishmayana S, Rahayu I, Eddy DR. Optimisation of Zinc Oxide Nanoparticle Biosynthesis Using Saccharomyces Cerevisiae with Box-Behnken Design. Revista de Chimie. 2021 September 07;72(1):78-88.
[56] Soni S, Patel T, Thakar B, Pandya V, Bharadia P. Nanosuspension: An approach to enhance solubility of drugs. IJPI's Journal of Pharmaceutics and Cosmetology. 2012;2(9):50-63.
[57] Zhang C, Liu J, Ahmeda A, Liu Y, Feng J, Guan H, Li C, Nowrozi M, Zangeneh MM, Zangeneh A, Almasi M. Biosynthesis of zinc nanoparticles using Allium saralicum RM Fritsch leaf extract; Chemical characterization and analysis of their cytotoxicity, antioxidant, antibacterial, antifungal, and cutaneous wound healing properties. Applied Organometallic Chemistry. 2020 Feb 24:e5564.
[58] Velsankar K, Sudhahar S, Parvathy G, Kaliammal R. Effect of cytotoxicity and aAntibacterial activity of biosynthesis of ZnO hexagonal shaped nanoparticles by Echinochloa frumentacea grains extract as a reducing agent. Materials Chemistry and Physics. 2020 Jan 1;239:121976.
[59] Chauhan P, Shrivastava V, Tomar R. Biosynthesis of zinc oxide nanoparticles using Cassia siamea leaves extracts and their efficacy evaluation as potential antimicrobial agent. Journal of Pharmacognosy and Phytochemistry. 2019;8(3):162-6.
[60] Ravichandran V, Sumitha S, Ning CY, Xian OY, Kiew Yu U, Paliwal N, Shah SA, Tripathy M. Durian waste mediated green synthesis of zinc oxide nanoparticles and evaluation of their antibacterial, antioxidant, cytotoxicity and photocatalytic activity. Green Chemistry Letters and Reviews. 2020 Apr 2;13(2):102-16.
[61] Sachdeva A, Singh S, Singh PK. Synthesis, characterisation and synergistic effect of ZnO nanoparticles to antimicrobial activity of silver nanoparticle. Materials Today: Proceedings. 2021 Jan 1;34:649-53.
[62] Dulta K, Koşarsoy Ağçeli G, Chauhan P, Jasrotia R, Chauhan PK. A novel approach of synthesis zinc oxide nanoparticles by bergenia ciliata rhizome extract: antibacterial and anticancer potential. Journal of Inorganic and Organometallic Polymers and Materials. 2021 Jan;31(1):180-90.
[63] Janaki AC, Sailatha E, Gunasekaran S. Synthesis, characteristics and antimicrobial activity of ZnO nanoparticles. Spectrochimica Acta Part A: Molecular and Biomolecular Spectroscopy. 2015 Jun 5;144:17-22.
[64] Narendra Kumar HK, Chandra Mohana N, Nuthan BR, Ramesha KP, Rakshith D, Geetha N, Satish S. Phyto-mediated synthesis of zinc oxide nanoparticles using aqueous plant extract of Ocimum americanum and evaluation of its bioactivity. SN Applied Sciences. 2019 Jun;1(6):1-9.
[65] Nithya K, Kalyanasundharam S. Effect of chemically synthesis compared to biosynthesized ZnO nanoparticles using aqueous extract of C. halicacabum and their

*e*ISSN1303-5150

antibacterial activity. OpenNano. 2019 Jan 1;4:100024.